Proceedings of the 2nd International Conference on Fluid Flow, Heat and Mass Transfer
Ottawa, Ontario, Canada, April 30 – May 1, 2015
Paper No. 149

Simulation of Al2O3-ATF Nanofluid in a Compact Heat Exchanger

Mohammed Ismail, Shahram Fotowat
University of Windsor
401 Sunset Avenue, Windsor, Ontario, Canada N9B 3P2
ismailf@uwindsor.ca; fotowat@uwindsor.ca

Amir Fartaj
University of Windsor, Department of Mechanical Automotive and Materials Engineering
401 Sunset Avenue, Windsor, Ontario, Canada N9B 3P2
fartaj@uwindsor.ca

Abstract- This research presents a numerical study on the heat transfer of automatic transmission fluid (ATF) with Aluminum Oxide (Al_2O_3) nanofluid in a multiport slab minichannel heat exchanger (MICHX) under laminar flow conditions. The MICHX test specimen with the test section is modeled and solved using a finite volume method based CFD code. Five different concentrations ranges from 1%-3%vol of Al_2O_3 nanofluids are considered in this study. Liquids of a steady temperature of 76°C are cooled through a constant air flow rate of 507g/s and temperature of 14°C in a cross-flow orientation. Different Reynolds numbers ranging from 50 to 210 are maintained for each volume concentration. Numerical results show higher pressure drop of nanofluid than that of ATF; it slightly increases with the increase of volume concentrations of nanoparticles. Results also show the enhanced heat transfer due to presence of the nanoparticles in the base fluid. The effects of volume fraction of nanoparticles on liquid-side heat transfer coefficient and Nusselt number (Nu) are computed. A general correlation of liquid-side Nu with Re is established and presented in this study.

***Keywords*:** Automatic transmission fluid, nanoparticles, nanofluid, numerical simulation, serpentine minichannel, multiport, aluminum oxide.

Nomenclature

ATF	automatic transmission fluid
C_p	specific heat, J/kgK
G	generations of TKE, J/kg, or m^2/s^2
h	heat transfer coefficient, w/m^2K
k	thermal conductivity, w/mK
$MICHX$	minichannel heat exchanger
Nu	Nusselt number
P	pressure, kPa
$\dot{Q}$	heat transfer rate, w
Re	Reynolds number
T	temperature, ℃
TKE	turbulence kinetic energy, J/kg, or m^2/s^2
u	fluid velocity, m/s

Greek symbols

$\emptyset$	volume fraction
μ	dynamic viscosity, Ns/m^2or kg/ms
ρ	density, kg/m^3
σ_k	turbulent Prandtl number for k
τ	shear stress, kg/ms^2
Subscripts	
bf	base fluid
f	fluid (liquid)
i, j, and k	x, y and z components respectively
nf	nanofluid
np	nanoparticle
t	turbulence

1. Introduction

Rapidly increased energy demands, space limitations, and materials savings are the key issues of everyday life, and thus a secured and available supply of energy is important for the sustainability and economic development (Khan and Fartaj 2011). More than 70% of energy, we are using today, is produced in or through the form of heat which needs to be transferred into a system or removed from the system. Enhanced heat transfer rate is a demanding challenge in rapid cooling and heating environment. In order to achieve the increased and faster heat transfer, Al2O3 nanoparticles suspensions in ATF are introduced due to the high thermal properties and large surface area of the nanoparticles. In addition, minichannel heat exchanger (MICHX) is employed to reduce the weight and increase the thermal performance. In automotive and industrial applications, miniature heat exchanger has been becoming more popular because of its increased heat transfer flux, lighter weight, and enhanced heat transfer area density compared with conventional one.

The use of nanoparticles in heat transfer field was first studied at the Argonne National laboratory by Choi and Eastman (1995). In order to overcome the low heat transfer properties of common fluids, it is essential to search for the solid particles having several hundred times higher thermal conductivities than those of conventional fluids as shown by Daungthongsuk and Wongwises (2007). It is claimed that nanofluids show superior stability, rheological properties, and thermal conductivities with no penalty in pressure drop compared with suspended mili-or-micro particles.

Improvement of convective heat transfer is reported by numerous researchers, including Heris et al (2014), Jung et al (2009), Dominic et al (2014), and Nourafkan et al (2014). Flow boiling heat transfer investigations are performed in laminar flow condition using low volume concentration of up to 170nm nanoparticles sizes. A heat transfer increment of up to 200% for Cu_2O and Al_2O_3/DI-water nanofluids compared to DI-water is established. However, it is claimed that the improvement and applications of nanofluids may be slowed down by several reasons e.g. long term stability, increasing pressure drop, and nanofluids' thermal performance in fully developed flow, lower specific heat of nanofluids, and greater cost of nanofluids preparation.

Many researchers, including Vajjha et al (2009), Hussein et al (2013), and Albadr et al (2013) investigated the enhancement of heat transfer and the influence of the density of nanofluids to the performance of some common nanofluids. The authors introduced Al_2O_3, CuO, TiO_2, and SiO_2 nanoparticles into a DI-water or an ethylene glycol and water mixture (60:40 by weight) in a variety of volume concentrations and sizes. Significantly increased Nusselt number and heat transfer coefficient of nanofluids are reported. The specific heat of Al_2O_3/water nanofluid is studied by Zhou et al (2008) and found that the specific heat of nanofluids decrease with increase of volume fraction of nanoparticles. Moreover, Barbes et al. (2012) conducted an experimental study on specific heat of Al_2O_3/water and ethylene glycol nanofluid at temperatures between 25℃ and 65℃ and and verified with the Hamilton–Crosser model.

Lee and Choi (1997) conducted an investigation to evaluate the thermal conductivity of γ-Al_2O_3 dispersed in water. The thermal conductivity of γ-Al_2O_3 is three times that of water, which allows nearly three-fold increases in heat fluxes of liquid nitrogen–cooled microchannel heat exchanger. In addition, the heat transfer coefficients of several graphitic nanofluids have been studied by Yang et al (2005) in a horizontal tube heat exchanger under laminar flow. They claimed that the nanoparticles improve the heat transfer coefficient of the fluid system in laminar flow. However, the improvement is found much lower than that of the predicted values obtained from the thermal conductivity correlations. The authors recommended to consider type of nanoparticles, particle loading, base fluid chemistry as well as the process temperature during preparation of nanofluids in order to improve heat transfer coefficients.

A theoretical study of the thermal conductivity of nanofuids is introduced by Xuan and Li (2000). They claimed that the nanofuids shows great potential in enhancing the heat transfer process. They stated that the volume fraction, shape, dimensions, and properties of the nanoparticles affect the thermal conductivity of nanofluids. Eastman et al (2001) stated that a ''nanofluid'' consisting of copper nanometer-sized particles dispersed in ethylene glycol has a higher effective thermal conductivity than either pure ethylene glycol or ethylene glycol containing the same volume fraction of dispersed oxide nanoparticles.

CuO nanoparticles in ethylene glycol/water (60:40) of 0% to 6.12% at temperature of −35℃ to 50℃ are studied by Namburu et al (2007). They stated that the viscosity of nanofluids decreases exponentially as the temperature increases. The relative viscosity of CuO nanofluids increases with the increase of %vol and decreases substantially with temperature for higher concentrations. Furthermore, Garg et al (2008) investigated the thermal conductivity and viscosity of 2%vol CuO nanoparticles in water/ethylene glycol and claimed that the thermal conductivity is twice that of the Maxwell model and the viscosity is about four times that of the predicted value of Einstein (1906) model. The viscosity and thermal conductivity of 21nm TiO2 nanoparticles in DI-water up to a volume fraction of 3% of particles at temperatures of up to 55℃ were also examined by Turgut et al (2009). They established that the thermal conductivity of the nanofluid increases with an increase of particle volume fraction, and the enhancement is observed to be 7.4% higher than the base fluid at 13℃. Moreover, Elçioğlu (2013) experimentally and analytically studied the viscosity of Al2O3/water nanofluid for different nanoparticle volumetric fractions, nanoparticle diameters, and temperatures. Their results showed that the viscosity of Al_2O_3/water nanofluids increases with the nanoparticle diameter and decreases exponentially with temperature. Experimental investigations are performed to determine the viscosity of TiO_2 and Al_2O_3 nanoparticles suspended in a mixture of ethylene glycol/water. Another experimental study at various volume fractions between 0% and 4% and a temperature range of 15℃–60℃ is conducted by Yiamsawas et al (2013). Results indicate that the theoretical models are not suitable to predict the viscosity of nanofluids.

Study on heat transfer and fluid flow characterization of ATF base Al_2O_3 nanofluid in narrow channels is very rare in open literatures. Therefore, the current study dealing with Al2O3/ATF nanofluid flow characteristics might supplement the useful information for industrial applications. The main purpose of this study is to evaluate the pressure drop and heat transfer characteristics of Al_2O_3/ATF nanofluid as a homogeneous single-phase fluid in a MICHX.

2. Numerical Method

The numerical simulation is performed in a serpentine slab multiport minichannel heat exchanger (MICHX) as shown in Fig. 1. The specifications of the MICHX are presented in Table. 1.

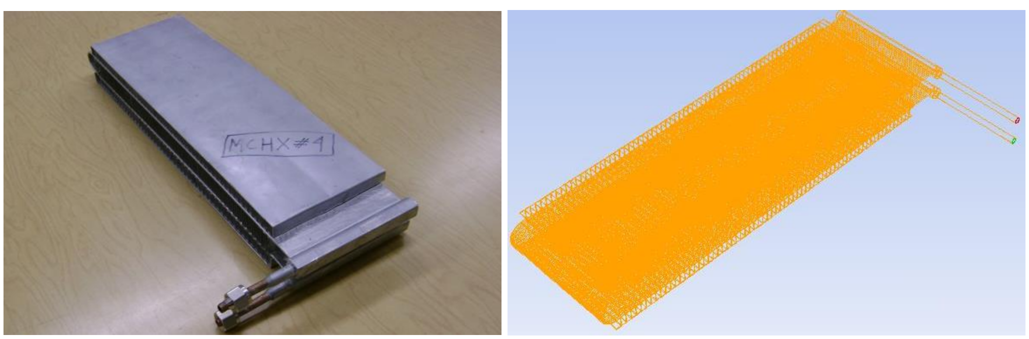

Fig. 1. Photograph (left) and Model (right) of MICHX used in current study

Table 1. Specifications of MICHX (Ismail et al 2013)

Parameters		Magnitudes
Materials of MICHX		Aluminum
Number of channels		68
Channel diameter		1 mm
Port to port distance		1.463 mm
Slab	length (x-axis)	304 mm
	thickness (y-axis)	2 mm
	width (z-axis)	100 mm

Parameters		Magnitudes
Inner diameter of serpentine curve		20 mm
Inner diameter of Header		4.76 mm
Fin	density	8 fins per 25.4 mm
	height: middle	20 mm
	height: top & bottom	10 mm
	thickness	0.1 mm

Assuming the base fluid and the nanoparticles are in thermal equilibrium, following time-averaged instantaneous governing equations are used to compute steady state and incompressible fluid flow without chemical reaction:

Continuity: $\frac{\partial}{\partial x_i}(\rho u_i) = 0$ (1)

Momentum: $\frac{\partial}{\partial x_i}(\rho u_i u_k) = \frac{\partial}{\partial x_i}\left(\mu \frac{\partial u_k}{\partial x_i}\right) - \frac{\partial P}{\partial x_i} + \frac{\partial}{\partial x_i}\left(-\rho \overline{u_i' u_j'}\right)$ (2)

Energy: $\frac{\partial}{\partial x_i}(\rho u_i T) = \frac{\partial}{\partial x_i}\left(\frac{K}{C_p}\frac{\partial T}{\partial x_i} + u_i(\tau_{ij})_{eff}\right)$ (3)

Turbulence kinetic energy: $\frac{\partial}{\partial x_i}(\rho k u_i) = \frac{\partial}{\partial x_i}\left[\left(\mu + \frac{\mu_t}{\sigma_k}\right)\frac{\partial k}{\partial x_i}\right] + G_k - \rho\varepsilon$ (4)

The following equations are used to compute the thermophysical properties of nanofluids:

Density (Pak and Cho 1998): $\rho_{nf} = \emptyset\rho_{np} + (1-\emptyset)\rho_{bf}$ (5)

Specific heat (Xuan and Roetzel 2000): $Cp_{nf} = \frac{\emptyset(\rho Cp)_{np} + (1-\emptyset)(\rho Cp)_{bf}}{\emptyset\rho_{np} + (1-\emptyset)\rho_{bf}}$ (6)

Thermal conductivity (Yu and Choi 2003): $k_{nf} = \left[\frac{k_{np} + 2k_{bf} + 2(k_{np} - k_{bf})\emptyset}{k_{np} + 2k_{bf} - (k_{np} - k_{bf})\emptyset}\right] k_{bf}$ (7)

Dynamic viscosity (Brinkman 1952): $\mu_{nf} = \mu_{bf}/(1 - \emptyset)^{2.5}$ (8)

Mass flow rates and temperature are specified at the inlet boundaries of both liquid and air. Inlet air mass flow rate of 507g/s is kept constant while inlet liquid flow rates are varied from 18.8g/s to 128g/s. Inlet temperatures of both air- and liquid-side are kept constant at 76°C and 14°C respectively. Temperature-dependent functions are used for thermophysical properties of ATF and nanofluids; whereas, constant properties are considered for air and aluminum. Outflow boundary condition is applied for at the outlet boundaries of both liquid and air. Adiabatic and no slip boundary conditions are specified at test chamber and serpentine walls.

2.1. Grid independency and validation

In order to validate the model, a numerical verification including a grid dependence study and an overall error in mass and heat balance is performed. The detail of the grid independency study is previously published (Ismail et al 2013) and is not repeated here. The overall error in mass and heat balance in all cases considered in this study is observed in a range of ±0.08% and ±0.36% respectively. In addition, a set of simulation results of water and glycol were compared with experimental results of Khan and Fartaj (2011) and found a very good agreement. These ensure that the model and results from the simulation are accurate and reliable.

3. Results and Discussions

3.1. Pressure drop (ΔP)

The effects of Reynolds number as well as volume fraction of nanoparticles on liquid-side pressure drop (ΔP_f) are shown in Fig 3.1. It shows that the pressure drop, ΔP_f increases with the increase of Re_f. The slope of ΔP_f of nanofluids is steeper than that of ATF. The pressure drop of nanofluids are increased by 13%-44% compared with that of base fluid for the Reynolds number of 50 to 210. It is also observed that there is no significant difference in ΔP_f among the nanofluids of 1.0% to 3.0%vol concentrations.

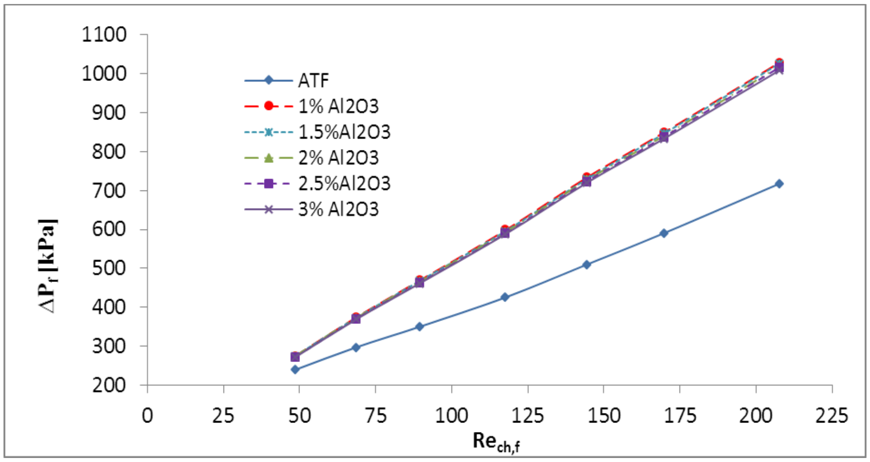

Fig. 3.1. Effects of Reynolds number as well as volume fraction of nanoparticles on liquid-side pressure drop

3.2. Heat transfer rate ($\dot{Q}$)

The effects of nanofluids on heat transfer rate ($\dot{Q}$) is demonstrated in Fig. 3.2. As expected, the heat transfer rate increases nonlinearly with the increase of liquid-side Reynolds (Re_f) number. At a particular Re_f, higher nanofluid concentration shows greater heat transfer rate due to its larger heat conduction compare to the base fluids. Moreover, the slop of $\dot{Q}$ is observed steeper at lower Re_f compared with those of higher Re_f. It is found that the heat transfer rate is increased by 1%-2%. For very low Reynolds number, especially for $Re_f \leq 100$, it is observed that there is no obvious variation of $\dot{Q}$ for the variation of volume concentration of nanoparticles. However, for $Re_f > 100$, higher heat transfer rate is observed for higher concentration.

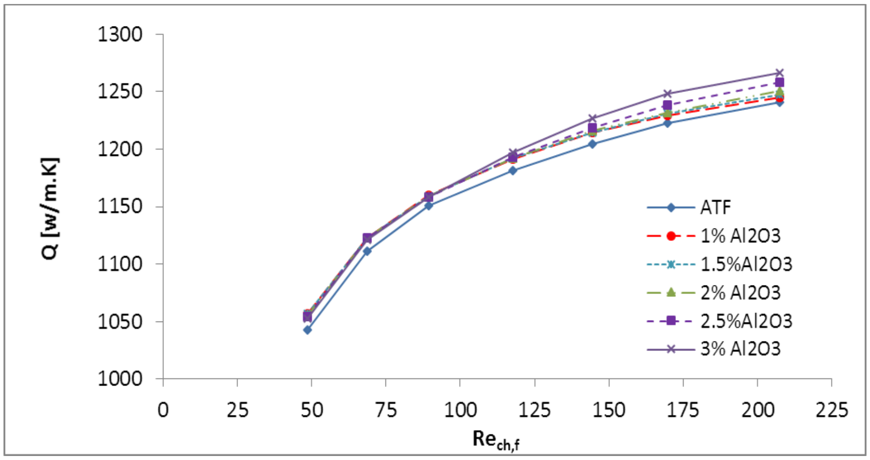

Fig. 3.2. Effects of Reynolds number as well as volume fraction of nanoparticles on heat transfer rate

3.3. Convective heat transfer coefficient (h_f)

The heat transfer coefficient is an important parameter for heat exchanger design. The liquid side heat transfer coefficient (h_f) vs Reynolds number (Re_f) for various nanofluid concentrations is illustrated in Fig. 3.3. It showed that h_f increases with the increase of Re_f, as expected. For a particular Re_f, h_f becomes slightly higher at higher concentration for the range of 1%≤∅≤3%.

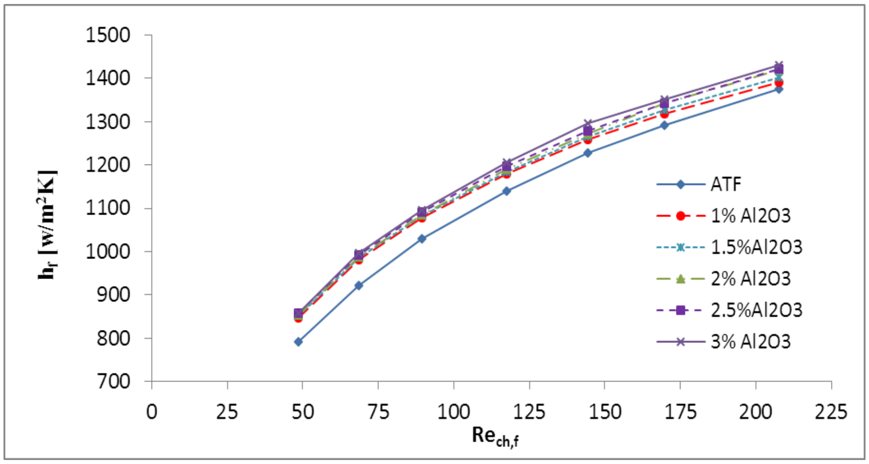

Fig. 3.3. Effects of Reynolds number as well as volume fraction of nanoparticles on heat transfer coefficient

3.4. Nusselt Number (Nu)

The heat transfer is generally stated in terms of Nusselt number (Nu) as a function of Reynolds number (Re) and Prandtl number (Pr). Fig. 3.4(a) shows the effect of liquid-side Re_f on Nu_f for nanofluid concentration from 1% to 3% at constant inlet liquid temperature of 76℃ and air temperature 14℃. It shows that the Nu_f increases nonlinearly with the increase of Re_f. The slop of Nu_f is found steeper at lower Re_f compared with those of higher Re_f. Nu_f is found to be higher for lower concentration because its thermal conductivity dominates the Nu_f compared with heat transfer coefficient of nanofluids. For Re_f≤100, Nu_{nf} is observed higher than Nu_{atf} because heat transfer coefficient of nanofluid dominates the Nusselt number. However, for Re_f>100, Nu_{nf} is lower than Nu_{atf} because thermal conductivity of nanofluid dominates the Nusselt number.

Fig. 3.4(b) shows the correlation of Nu_{nf}, Re_{nf}, and Pr_{nf}. From a nonlinear regression analysis (NLREG), an overall correlation of Nu_{nf}-Re_{nf}-Pr_{nf} is obtained in the form of $Nu_{nf}=0.23Re_{nf}^{0.37}Pr_{nf}^{1/3}$ for the range 50≤Re_{nf}≤210 for nanoparticles concentration levels from 1% to 3% as shown in Fig. 3.4(b).

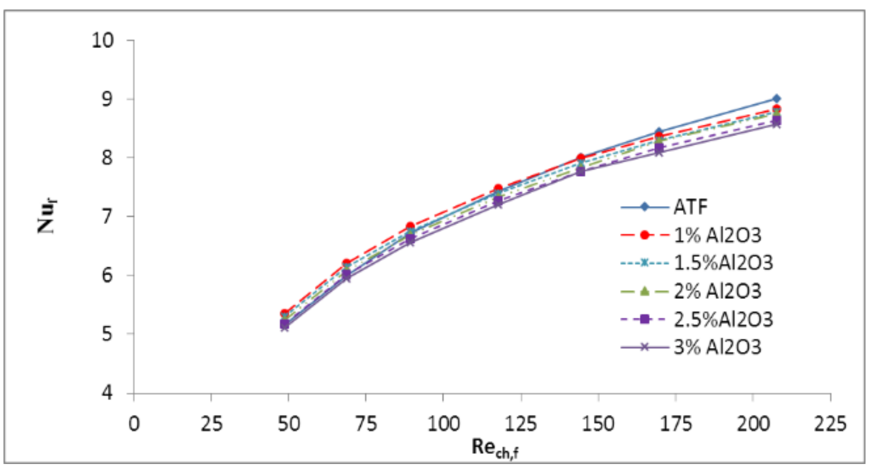

Fig. 3.4(a). Effects of Re_f on Nu_f

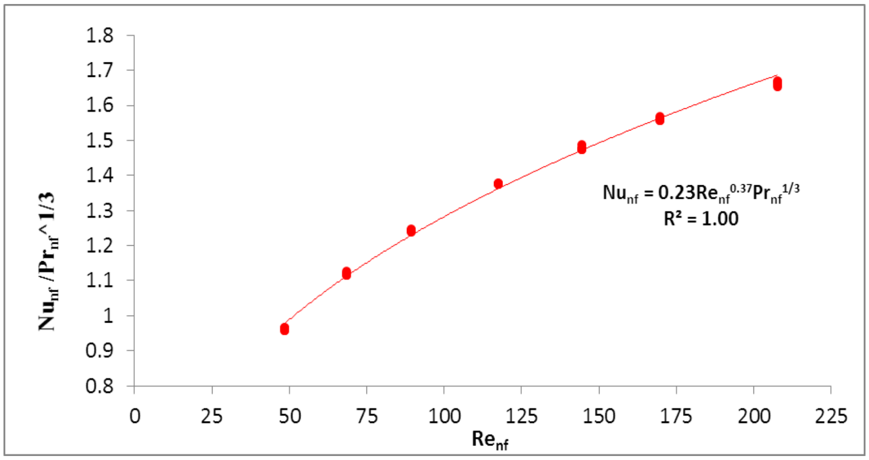

Fig. 3.5(b). Correlation of Nu_{nf}-Re_{nf}-Pr_{nf}

4. Conclusions

In this study, Reynolds number of liquids (ATF and Al_2O_3/ATF nanofluids) are varied from 50 to 210 for nanofluid concentration of $1\% \leq \emptyset \leq 3\%$. The inlet temperatures of liquid and air are kept constant at 76℃ and 14℃ respectively in all simulations. The investigation is conducted in a multiport slab minichannel heat exchanger. The pressure drop of nanofluid is increased by 13%-44% than ATF; it increases slightly with the increase of volume concentrations of nanoparticles. The heat transfer rate rises nonlinearly with the rise of Re_f. 1%-2% enhancement of $\dot{Q}$ is observed due to larger heat conduction compare to the base fluids. It is steeper at lower Re_f than those of higher Re_f. For Re_f>100, at a particular Re_f, heat transfer rate as well as heat transfer coefficient of fluids are higher for larger concentration of nanoparticles. As it is expected, h_f increases with the increase of Re_f. In addition, for $Re_f \leq 100$, Nu_{nf} is found higher than Nu_{atf} because of its dominating heat transfer coefficient. For Re_f>100, Nu_{nf} is lower than Nu_{atf} due to its dominating thermal conductivity. A general correlation of Nu_{nf}-Re_{nf}-Pr_{nf} is achieved in the form of $Nu_{nf}=0.23Re_{nf}^{0.37}Pr_{nf}^{1/3}$ from a nonlinear regression analysis.

References

Albadr J., Tayal S., Alasadi M. (2013). Heat transfer through heat exchanger using Al2O3 nanofluid at different concentrations. *Case Studies in Thermal Engineering*, 1, 38-44.

Barbe´s B., Pa´ramo R., Blanco E., Pastoriza-Gallego M.J., Pin˜ eiro M.M., Legido j.L., Casanova C. (2013). Thermal conductivity and specific heat capacity measurements of Al2O3 nanofluids. *J Therm Anal Calorim*, 111, 1615-1625.

Brinkman H.C. (1952). The viscosity of concentrated suspensions and solutions. *The Journal of Chemical Physics*, 20, 571.

Choi, S.U.S. and Eastman, J.A. (1995). Enhancing thermal conductivity of fluids with nanoparticles, Argonne National Laboratory, Argonne, IL, USA.

Eastman J.A., Choi S.U.S., Li S., Yu W., Thompson L.J. (2001). Anomalou effective thermal conductivities of ethylene glycol-based nanofluids containing copper nanoparticles. *Applied Physics Letters*, 78(6), 718-720.

Einstein A. (1906). A new determination of molecular dimensions. *Annln Phys.*, 19, 289 (and 34, 591).

Elçioğlu E. B. (2013). Experimental and theoretical investigations on alumina–water nanofluid viscosity with statistical analysis. MASc. Thesis, Middle East Technical University, Turkey.

Garg J., Poudel B., Chiesa M., Gordon J.B., Ma J.J., Wang J.B., Ren Z.F., Kang Y.T., Ohtani H., Nanda J., McKinley G.H., Chen G. (2008). Enhanced thermal conductivity and viscosity of copper nanoparticles in ethylene glycol nanofluid. *Journal of Applied Physics*, 103, 074301-1 – 074301-6.

Heris S.Z., Edalati, Z., Noie, S.H., and Mahian, O. (2014). Experimental iInvestigation of Al2O3/Water nanofluid through equilateral triangular duct with constant wall heat flux in laminar flow. *Heat Transfer Engineering*, 35, 1173–1182.

Hussein A.M., Sharma K.V., Bakar R.A., Kadirgama K. (2013). The effect of nanofluid volume concentration on heat transfer and friction factor inside a horizontal tube. *Journal of Nanomaterials*, 2013, ID 859563, 1-12.

Ismail M., Fartaj A., Karimi M. (2013). Numerical investigation on heat transfer and fluid flow behaviors of viscous fluids in a minichannel heat exchanger. *Numerical Heat Transfer*, Part A, 64, 1–29.

Jung J-Y., Oh H-S., Kwak H-Y. (2009). Forced convective heat transfer of nanofluids in microchannels. *International Journal of Heat and Mass Transfer*, 52, 466-472.

Khan M.G, Fartaj A. (2011). A review on microchannel heat exchangers and potential applications. *International Journal of Energy Research*, 35, 553–582

Lee S., Choi S.U.S. (1996). Application of metallic nanoparticles suspensions in advanced cooling systems "Proc. of 1996 Int. Mechanical Engineering Congress and Exhibition," Atlanta, GA (United States), Nov 17-22, ANL/ET/CP-90558; CONF-961105-20.

Namburu P.K., Kulkarnia D.P., Misrab D., Dasa D.K. (2007). Viscosity of copper oxide nanoparticles dispersed in ethylene glycol and water mixture. *Experimental Thermal and Fluid Science*, 32, 397-402.

Nourafkan E., Karimi G., Moradgholi J. (2013). Experimental study of laminar convective heat transfer and pressure drop of cuprous oxide/water nanofluid inside a circular tube. *Experimental Heat Transfer*, 28, 58-68.

Pak B.C., Cho Y.I. (1998). Hydrodynamic and heat transfer study of dispersed fluids with submicron metallic oxide particles. *Experimental Heat Transfer*, 11, 151-170.

Turgut A., Tavman I., Chirtoc M., Schuchmann H.P., Sauter C., Tavman S. (2009). Thermal conductivity and viscosity measurements of water-based TiO2 nanofluids. *Int. J. Thermophys*, 30, 1213–1226.

Vajjha R.S., Das D.K. (2009). Specific heat measurement of three nanofluids and development of new correlations. *Journal of Heat Transfer*, 131, 071601-1 – 071601-7.

Xuan Y., Li Q. (2000). Heat transfer enhancement of nanofluids. Int. J. Heat and Fluid Flow, 21, 58-64.

Xuan Y., Roetzel W. (2000). Conceptions for heat transfer correlation of nanofluids. *International Journal of Heat and Mass Transfer*, 43, 3701-3707.

Yang Y., Zhang G.Z., Grulke E.A., Anderson W.B., Wu G. (2005). Heat transfer properties of nanoparticle-in-fluid dispersions (nanofluids) in laminar flow. *International Journal of Heat and Mass Transfer*, 48, 1107-1116.

Yiamsawas T., Mahian O., Dalkilic A.S., Kaewnai S., Wongwises S. (2013). Experimental studies on the viscosity of TiO2 and Al2O3 nanoparticles suspended in a mixture of ethylene glycol and water for high temperature applications. *Applied Energy*, 111, 40-45.

Yu W., Choi S.U.S. (2003). The role of interfacial layers in the enhanced thermal conductivity of nanofluids: A Renovated Maxwell Model. *Journal of Nanoparticle Research*, 5, 167-171.

Zhou S-Q., Ni R. (2008). Measurement of the specific heat capacity of water-based Al2O3 nanofluid. *Applied Physics Letters*, 92, 093123-1 – 093123-3.